

Exciton recombination at crystal-phase quantum rings in GaAs/In_xGa_{1-x}As core/multishell nanowires

P. Corfdir, R. B. Lewis, O. Marquardt, H. Küpers, J. Grandal, E. Dimakis, A. Trampert, L. Geelhaar, O. Brandt, and R. T. Phillips

Citation: *Appl. Phys. Lett.* **109**, 082107 (2016); doi: 10.1063/1.4961245

View online: <https://doi.org/10.1063/1.4961245>

View Table of Contents: <http://aip.scitation.org/toc/apl/109/8>

Published by the [American Institute of Physics](#)

Articles you may be interested in

[Coaxial GaAs-AlGaAs core-multishell nanowire lasers with epitaxial gain control](#)

Applied Physics Letters **108**, 011108 (2016); 10.1063/1.4939549

[Radial tunnel diodes based on InP/InGaAs core-shell nanowires](#)

Applied Physics Letters **110**, 113501 (2017); 10.1063/1.4978271

[Impact of surfaces on the optical properties of GaAs nanowires](#)

Applied Physics Letters **97**, 201907 (2010); 10.1063/1.3519980

[Strain in semiconductor core-shell nanowires](#)

Journal of Applied Physics **106**, 053508 (2009); 10.1063/1.3207838

[Plan-view transmission electron microscopy investigation of GaAs/\(In,Ga\)As core-shell nanowires](#)

Applied Physics Letters **105**, 121602 (2014); 10.1063/1.4896505

[Residual strain and piezoelectric effects in passivated GaAs/AlGaAs core-shell nanowires](#)

Applied Physics Letters **102**, 191103 (2013); 10.1063/1.4803685

MMR TECHNOLOGIES

**THE WORLD'S RESOURCE FOR
VARIABLE TEMPERATURE
SOLID STATE CHARACTERIZATION**

WWW.MMR-TECH.COM

OPTICAL STUDIES SYSTEMS SEEBECK STUDIES SYSTEMS MICROPROBE STATIONS HALL EFFECT STUDY SYSTEMS AND MAGNETS

The advertisement displays a variety of scientific instruments used for solid state characterization, including optical studies systems, Seebeck studies systems (models SB1000 and K2000), microprobe stations, and Hall effect study systems and magnets (models HS000 and K2000).

Exciton recombination at crystal-phase quantum rings in GaAs/In_xGa_{1-x}As core/multishell nanowires

P. Corfdir,^{1,a)} R. B. Lewis,¹ O. Marquardt,¹ H. Küpers,¹ J. Grandal,^{1,b)} E. Dimakis,^{1,c)}
 A. Trampert,¹ L. Geelhaar,¹ O. Brandt,¹ and R. T. Phillips²

¹Paul-Drude-Institut für Festkörperelektronik, Hausvogteiplatz 5–7, 10117 Berlin, Germany

²Cavendish Laboratory, University of Cambridge, J. J. Thomson Avenue, Cambridge CB3 0HE, United Kingdom

(Received 3 June 2016; accepted 3 August 2016; published online 26 August 2016)

We study the optical properties of coaxial GaAs/In_xGa_{1-x}As core/multishell nanowires with x between 0.2 and 0.4 at 10 K. The evolution of the photoluminescence energy of the In_xGa_{1-x}As quantum well shell with x and shell thickness agrees with the result of 8-band $\mathbf{k} \cdot \mathbf{p}$ calculations, demonstrating that the shell growth is pseudomorphic. At low excitation power, the photoluminescence from the shell is dominated by the recombination of exciton states deeply localized within the shell. We show that these states are associated with crystal-phase quantum rings that form at polytype segments of the In_xGa_{1-x}As quantum well shell. *Published by AIP Publishing.* [<http://dx.doi.org/10.1063/1.4961245>]

Semiconductor nanowires of coaxial core and multishell geometry enable coherent heterostructures with lattice mismatch exceeding the limits found for planar layered structures,¹ and thereby offer more flexibility in bandgap engineering via strain or quantum confinement. Epitaxial shells also strongly reduce the impact of surface recombination at the nanowire sidewalls, making it possible to realize group-III-arsenide-based nanowire heterostructures for optoelectronic applications in the near-infrared range operating at room temperature.^{2–4} However, GaAs nanowires are also characterized by high densities of twins, stacking faults and wurtzite/zincblende (WZ/ZB) polytype segments. These so-called crystal-phase quantum structures localize charge carriers at low temperatures, giving rise to intense transitions in the photoluminescence (PL) spectra of the nanowires.^{5–7}

In this letter, we study the optical properties of GaAs/In_xGa_{1-x}As core/multishell nanowires by PL and photoluminescence excitation (PLE) spectroscopy at 10 K. The PL of the In_xGa_{1-x}As quantum well (QW) shell consists of two bands that redshift with increasing shell thickness and x . The band at higher energy arises from the In_xGa_{1-x}As QW exciton, and the one at lower energy comes from exciton recombination at crystal-phase quantum rings (QRs) formed at the intersection of the radial In_xGa_{1-x}As QW with an axial polytype segment.

GaAs/In_xGa_{1-x}As/GaAs core/shell/shell nanowires were grown by molecular beam epitaxy on Si(111) substrates covered by their native oxide. GaAs nanowire cores with a length of 3–4 μm were grown with a density of about 0.1–1 μm^{-2} by Ga-assisted vapor-liquid-solid growth. The Ga droplets were consumed by exposure to As, and subsequently, GaAs, In_xGa_{1-x}As, and GaAs shells were grown around the GaAs cores (see Ref. 2 for further details). The thickness (L) and In content (x) of the In_xGa_{1-x}As shell were varied between 10

and 35 nm and 0.2 and 0.4, respectively. The microstructure of the core/multishell nanowires was investigated by transmission electron microscopy (TEM).

Photoluminescence experiments were performed using a Ti:sapphire laser emitting at 1.64 eV. The laser light was focused down to a 50 μm diameter spot, and the PL signal was dispersed with a double spectrometer and detected with either a charge-coupled device (CCD) or an (In,Ga)As array. Micro-PL and -PLE experiments were performed with a Ti:sapphire laser continuously tunable between 1.3 and 1.7 eV and focused down to a 1.5 μm diameter spot. The laser power and wavelength were monitored using an (In,Ga)As photodiode and a high finesse Fizeau interferometer, respectively. The PL signal was sent to a triple spectrometer working in subtractive mode and detected with a CCD. Both PL and PLE experiments were carried out at 10 K in backscattering geometry on ensembles of nanowires.

Figures 1(a)–1(c) show the excitation power dependence of the PL spectra from ensembles of GaAs/In_xGa_{1-x}As core/shell nanowires with various L and x at 10 K. At low excitation powers, the spectrum for the sample with $x = 0.2$ and $L = 10$ nm consists of a broad transition centered at 1.35 eV [Fig. 1(a)]. On the low-energy side of this band, one detects a series of weaker transitions with full-width at half maximum down to 1 meV. While the band at 1.35 eV broadens and slightly blueshifts with increasing excitation power, the series of narrow transitions at lower energies develops into a broad band that saturates at the highest powers. The energy of the latter band is indicated by a grey arrow in Fig. 1(a). Qualitatively similar behaviors are observed for the samples with larger x and L [Figs. 1(b) and 1(c)]. Figure 1(d) shows that the high-energy band observed in Figs. 1(a)–1(c) under high excitation redshifts with increasing x and L , indicating that it arises from the recombination of free excitons confined in the In_xGa_{1-x}As shells. The energy of the band at lower energy follows a similar dependence on x and L , and we thus attribute it to the recombination of localized excitons in the In_xGa_{1-x}As shells [Figs. 1(a)–1(c)]. Radiative recombination in either the GaAs core or outer shell would be

^{a)}Electronic mail: corfdir@pdi-berlin.de

^{b)}Current address: Departamento de Ingeniería Electrónica and ISOM, ETSI Telecomunicación, Universidad Politécnica, 28040 Madrid, Spain.

^{c)}Current address: Helmholtz-Zentrum Dresden-Rossendorf, Bautzner Landstraße 400, 01328 Dresden, Germany.

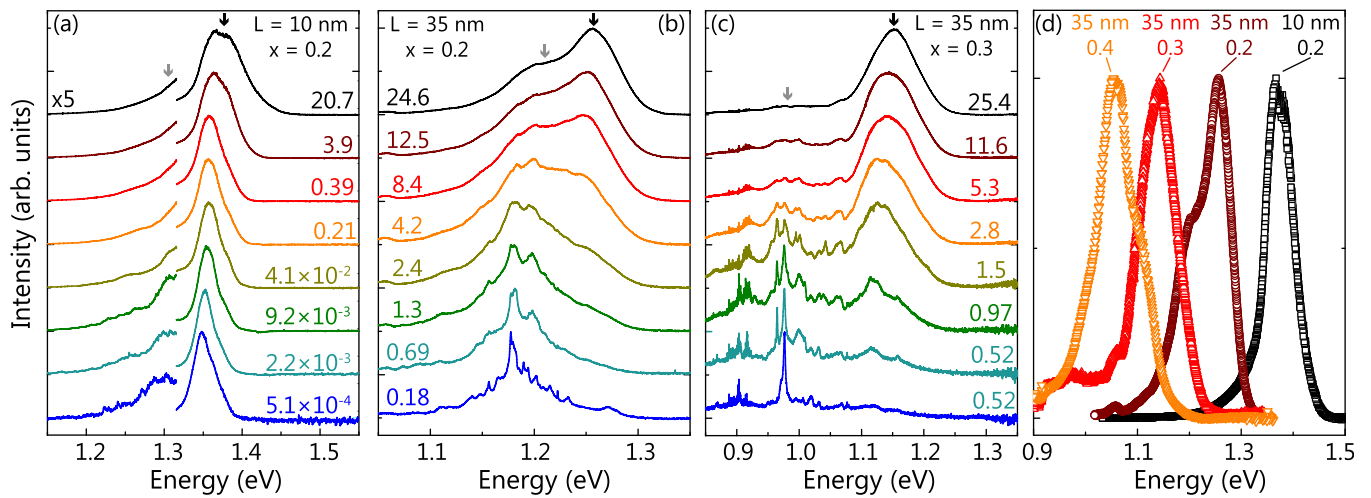


FIG. 1. Excitation power dependence of the PL spectra of GaAs/In_xGa_{1-x}As nanowires ensembles at 10K with (a) $L = 10$ nm and $x = 0.2$ and [(b), (c)] $L = 35$ nm and $x = 0.2$ (b) and 0.3 (c). The excitation power in mW is specified on each spectrum. The spectra are normalized and shifted vertically for clarity. The black and grey arrows in (a)–(c) highlight the energies of the emission bands related to free and localized excitons, respectively, which were obtained by a deconvolution of the PL spectra. (d) Normalized PL spectra of samples with various x and L under high excitation at 10K.

expected above 1.45 eV, but no transition is observed in this spectral range [Fig. 1(a)]. This finding differs from results reported for GaAs/(Al,Ga)As core/shell nanowires⁸ and indicates that the transfer of excitons from the binary GaAs core and outer shell to the (In,Ga)As QW is more efficient than for the ternary alloy (Al,Ga)As.

Figure 2 shows a comparison of the experimental results and those of an 8-band $\mathbf{k} \cdot \mathbf{p}$ model of the electronic states as a function of x for $L = 10$ and 35 nm; this confirms that the PL spectra in Fig. 1(d) are dominated by the recombination of free excitons in the In_xGa_{1-x}As shell. For these calculations, we assume the nanowires to have a zincblende structure, we use the set of material parameters proposed in Ref. 9, and we include Coulomb interaction.¹⁰ The strain state distribution in the nanowire, obtained by numerical minimization of the elastic strain energy, depends on x and on the dimensions of the core and the shells.¹¹ Even though the strain state is different at the center of the facets and at the edge between two facets, the electron and hole

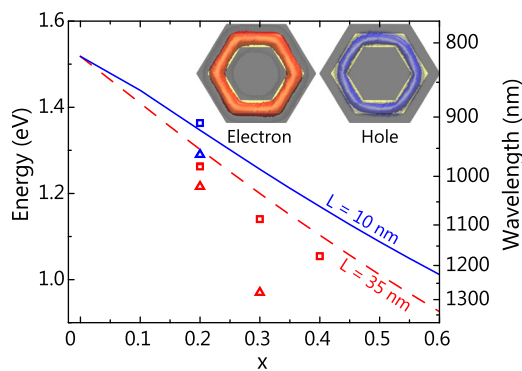


FIG. 2. PL energy as a function of x of the free (squares) and localized (triangles) excitons in the 10 and 35 nm thick In_xGa_{1-x}As shell QWs (blue and red symbols, respectively). The ground-state exciton energies obtained from 8-band $\mathbf{k} \cdot \mathbf{p}$ calculations for purely zincblende GaAs/In_xGa_{1-x}As core/shell nanowires with $L = 10$ and 35 nm are shown by solid and dashed lines, respectively. The inset shows the electron (red) and hole (blue) ground-state charge densities in the nanowires with $L = 10$ nm and $x = 0.2$. The thickness of the GaAs outer shell has been reduced for clarity.

wavefunctions of the exciton ground state are mostly delocalized across the shell (inset of Fig. 2). The good agreement between the evolution of the measured and computed PL energies with increasing x and L shows that the growth of the shell remains pseudomorphic up to $x = 0.4$.

The exciton localization energy in the QW shell is obtained from the difference between the emission energies of free and localized excitons. At low temperatures and excitation powers, excitons in the In_xGa_{1-x}As shell are probably localized at fluctuations in L . As can be easily seen in Fig. 2, for a given x , monolayer fluctuations in L cannot account for the exciton localization energies of 74, 47, and 170 meV observed in Figs. 1(a)–1(c), respectively. Moratis *et al.*¹² reported for GaAs/In_xGa_{1-x}As core/shell nanowires with an average x of 0.015 and L ranging between 5 and 50 nm the observation of narrow transitions similar to the ones observed in Figs. 1(a)–1(c) at low excitation powers, which they attributed to exciton localization at In-rich clusters. However, the presence of such clusters has been excluded by the TEM investigation in Ref. 13, which revealed that the In distribution along the In_xGa_{1-x}As shell facet is uniform.

We have so far ruled out that fluctuations in L , x , and strain state could be at the origin of the localized states giving rise to the transitions observed in Figs. 1(a)–1(c) at low excitation powers. The bright-field TEM image in Fig. 3(a) indicates that the GaAs cores of our nanowires are composed of segments with alternating ZB/WZ lattice structures and/or exhibit high densities of twins and stacking faults, as it is typically observed in this type of nanowire.⁵ These crystallographic defects, which we refer to as crystal-phase quantum structures, act as QWs¹⁴ that efficiently localize excitons along the nanowire axis.^{5,7,15} It is clear from Fig. 3(a) that the crystal-phase QWs formed during the axial growth of the GaAs core extend into the shells. Therefore, as depicted in Fig. 3(b), the intersection between the In_xGa_{1-x}As shell QW and the crystal-phase QW perpendicular to the nanowire axis gives rise to a ring structure, which we refer to as a crystal-phase quantum ring. The formation of optically active quantum wires at the intersection between a stacking fault and a

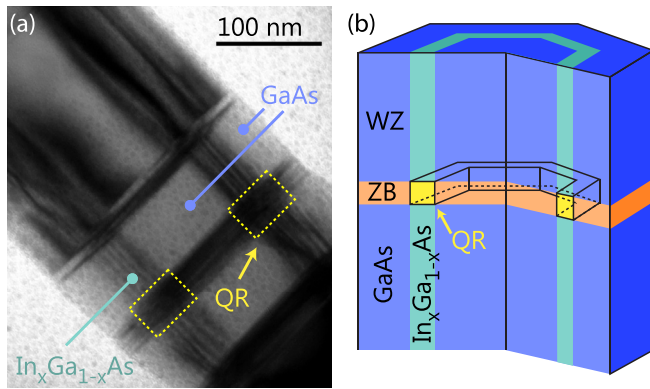


FIG. 3. (a) Bright-field TEM image of a nanowire with $L=11$ nm and $x=0.2$. The contrast variation along the nanowire axis is due to twins and an alternation between ZB and WZ lattice structures. The formation of quantum rings (QR) is highlighted by the rectangles. (b) Schematic representation of the formation in a core/shell nanowire of a crystal-phase QR (yellow region) at the intersection between an $\text{In}_x\text{Ga}_{1-x}\text{As}$ shell QW and a ZB/WZ crystal-phase QW.

QW has been reported previously for nonpolar III-nitride planar heterostructures.^{16,17} We propose that crystal-phase quantum rings are responsible for the band of localized exciton states observed in Fig. 1. Since the band alignment between the WZ and ZB phases of a III-V semiconductor is type II, the ring depicted in Fig. 3(b) acts as a well for electrons and as a barrier for holes. As the conduction and valence band offsets between WZ and ZB $\text{In}_x\text{Ga}_{1-x}\text{As}$ are small,¹⁸ the squared modulus of the electron-hole overlap integral for an exciton in a crystal-phase quantum ring is close to one, consistent with the observation that optical transitions related to quantum rings are strong (Fig. 1).

To investigate the dynamics of excitons in GaAs/ $\text{In}_x\text{Ga}_{1-x}\text{As}$ core/multishell nanowires with crystal-phase quantum rings, we have performed micro-PL and micro-PLE experiments on the sample with a 10 nm thick $\text{In}_{0.2}\text{Ga}_{0.8}\text{As}$ shell. Figure 4(a) shows a micro-PL spectrum taken on this sample. Although only a few nanowires are probed in this experiment, one can still differentiate between transitions related to the recombination of free QW excitons and excitons in crystal-phase quantum rings. The evolution of the PL

intensity at 1.345 eV with increasing excitation energy between 1.37 and 1.53 eV is also displayed in Fig. 4(a). In agreement with the results in Refs. 19–21, the strong increase in the PL intensity for excitation energies above 1.50 eV arises from the generation of carriers in segments of the GaAs core and outer shell, free of twins and stacking faults, followed by their transfer to the (In,Ga)As shell where they recombine radiatively. For energies larger than 1.49 eV, the dependence of the PL intensity I on the energy of the excitation laser E is well reproduced using a logistic function²²

$$I(E) \propto (1 + \exp[(E - E_0)/\Delta E])^{-1}, \quad (1)$$

where E_0 and ΔE are the energy and the broadening of the absorption edge, respectively. Fitting the PLE scan taken at 1.345 eV [(1) in Fig. 4(a)], we obtain $E_0 = 1.509$ eV and $\Delta E = 9$ meV. Figure 4(b) shows that E_0 and ΔE depend on the exact detection energy. For instance, E_0 ranges between 1.508 and 1.520 eV for detection energies between 1.30 and 1.42 eV, and exhibits an average value of 1.514 eV. These fluctuations in the value of E_0 arise partly from the fact that absorption in WZ and ZB GaAs nanowire segments occurs at slightly different energies.¹⁹ Wire-to-wire inhomogeneities in x and L responsible for the inhomogeneous broadening of the PL from the free QW exciton PL in Fig. 1 also induce strain fluctuations in the GaAs core and outer shells that cause the variations in E_0 seen in Fig. 4(b).

Absorption bands labeled (2) and (3) and about 10 and 100 times weaker than (1), respectively, are also observed in Fig. 4(a). Fitting these bands with Eq. (1) yields $E_0 = 1.451$ and 1.398 eV for bands (2) and (3), respectively. Since crystal-phase QWs exhibit a two dimensional density of states¹⁴ and can be found in high densities in the GaAs core and outer shell of our nanowires [Fig. 3(a)], we attribute band (2) to the generation of charge carriers in the polytypic GaAs core and outer shell followed by their capture and radiative recombination in the $\text{In}_x\text{Ga}_{1-x}\text{As}$ QW and crystal-phase quantum rings. Note that the average difference in E_0 between fault-free and polytype GaAs nanowire segments is 62 meV, suggesting that carrier generation occurs at nanowire segments with frequent alternation between WZ and ZB

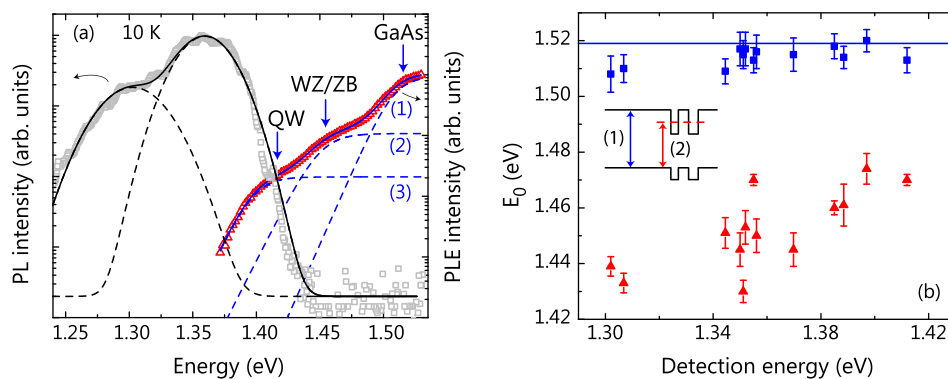


FIG. 4. (a) PL (squares, left axis) and PLE spectra taken at 1.345 eV (triangles, right axis) of the nanowires with $L = 10$ nm and $x = 0.2$ at 10 K. The black solid line is a fit to the PL spectrum with two Gaussians centered at 1.303 and 1.360 eV (dashed lines). The blue solid line is a fit to the PLE scan using three logistic functions (blue dashed lines) accounting for absorption from (1) GaAs fault-free segments, (2) polytype GaAs segments, and (3) the $\text{In}_x\text{Ga}_{1-x}\text{As}$ shell QW (also highlighted by arrows). (b) The absorption edge E_0 for GaAs fault-free and polytype segments (squares and triangles, respectively) plotted as a function of the detection energy. The linewidths ΔE are shown graphically by the error bars. The line indicates the bandgap of strain-free ZB GaAs. Inset: transitions related to (1) fault-free and (2) polytype nanowire segments.

structures rather than at isolated stacking faults.⁵ This energy difference is also close to the 48 meV energy difference between the QW free excitons and deeply localized states in the samples with $L = 35$ nm and $x = 0.2$ (Fig. 2), confirming that these localized states arise from the crystal-phase quantum rings forming at polytype segments of the $\text{In}_x\text{Ga}_{1-x}\text{As}$. Finally, the absorption band labeled (3) in Fig. 4(a) is due to direct absorption in the $\text{In}_x\text{Ga}_{1-x}\text{As}$ shell QW.

In conclusion, we have investigated the optical properties of GaAs/ $\text{In}_x\text{Ga}_{1-x}\text{As}$ core/multishell nanowires at low temperature using PL and PLE spectroscopies. Recombination of excitons in both fault-free and polytype $\text{In}_x\text{Ga}_{1-x}\text{As}$ shell segments has been observed. The emission from polytype $\text{In}_x\text{Ga}_{1-x}\text{As}$ shell segments blueshifts with increasing confinement, indicating that they act as crystal-phase quantum rings. Light emission at $1.3 \mu\text{m}$ is observed for quantum rings with x values as low as 0.3, which makes crystal-phase quantum rings potentially attractive for the realization of light emitters in the $1.3 \mu\text{m}$ telecom range. The one-dimensional density of states of charge carriers in these rings²³ could be interesting for future low threshold lasers²⁴ or high-gain excitonic lasers.²⁵

We thank Chiara Sinito for carefully reading our manuscript. P.C. acknowledges funding from the Fonds National Suisse de la Recherche Scientifique through Project No. 161032. Additional funding from the Deutsche Forschungsgemeinschaft (Grant No. Ge2224/2-2) and from the EPSRC (Grant No. EP/C009200/01) is also acknowledged.

- ¹O. Salehzadeh, K. L. Kavanagh, and S. P. Watkins, *J. Appl. Phys.* **114**, 054301 (2013).
- ²E. Dimakis, U. Jahn, M. Ramsteiner, A. Tahraoui, J. Grandal, X. Kong, O. Marquardt, A. Trampert, H. Riechert, and L. Geelhaar, *Nano Lett.* **14**, 2604 (2014).
- ³J. Treu, T. Stettner, M. Watzinger, S. Morkötter, M. Döblinger, S. Matich, K. Saller, M. Bichler, G. Abstreiter, J. J. Finley, J. Stangl, and G. Koblmüller, *Nano Lett.* **15**, 3533 (2015).
- ⁴K. Komolibus, A. C. Scofield, K. Gradkowski, T. J. Ochalski, H. Kim, D. L. Huffaker, and G. Huyet, *Appl. Phys. Lett.* **108**, 061104 (2016).

- ⁵M. Heiss, S. Conesa-Boj, J. Ren, H.-H. Tseng, A. Gali, A. Rudolph, E. Uccelli, F. Peiró, J. R. Morante, D. Schuh, E. Reiger, E. Kaxiras, J. Arbiol, and A. Fontcuberta i Morral, *Phys. Rev. B* **83**, 045303 (2011).
- ⁶P. Corfdir, B. Van Hattem, E. Uccelli, S. Conesa-Boj, P. Lefebvre, A. Fontcuberta i Morral, and R. T. Phillips, *Nano Lett.* **13**, 5303 (2013).
- ⁷A. V. Senichev, V. G. Talalaev, I. V. Shtrom, H. Blumtritt, G. E. Cirlin, J. Schilling, C. Lienau, and P. Werner, *ACS Photonics* **1**, 1099 (2014).
- ⁸P. Corfdir, H. Küpers, R. B. Lewis, T. Flissikowski, H. T. Grahn, L. Geelhaar, and O. Brandt, e-print [arXiv:1603.01111](https://arxiv.org/abs/1603.01111).
- ⁹A. Schliwa, M. Winkelkemper, and D. Bimberg, *Phys. Rev. B* **76**, 205324 (2007).
- ¹⁰O. Stier, M. Grundmann, and D. Bimberg, *Phys. Rev. B* **59**, 5688 (1999).
- ¹¹J. Grönqvist, N. Søndergaard, F. Boxberg, T. Guhr, S. Åberg, and H. Q. Xu, *J. Appl. Phys.* **106**, 053508 (2009).
- ¹²K. Moratis, S. L. Tan, S. Germanis, C. Katsidis, M. Androulidaki, K. Tsagaraki, Z. Hatzopoulos, F. Donatini, J. Cibert, Y. M. Niquet, H. Mariette, and N. T. Pelekanos, *Nanoscale Res. Lett.* **11**, 176 (2016).
- ¹³J. Grandal, M. Wu, X. Kong, M. Hanke, E. Dimakis, L. Geelhaar, H. Riechert, and A. Trampert, *Appl. Phys. Lett.* **105**, 121602 (2014).
- ¹⁴P. Corfdir, C. Hauswald, J. K. Zettler, T. Flissikowski, J. Lähnemann, S. Fernández-Garrido, L. Geelhaar, H. T. Grahn, and O. Brandt, *Phys. Rev. B* **90**, 195309 (2014).
- ¹⁵A. M. Graham, P. Corfdir, M. Heiss, S. Conesa-Boj, E. Uccelli, A. Fontcuberta i Morral, and R. T. Phillips, *Phys. Rev. B* **87**, 125304 (2013).
- ¹⁶T. J. Badcock, P. Dawson, M. J. Kappers, C. McAleese, J. L. Hollander, C. F. Johnston, D. V. S. Rao, A. M. Sanchez, and C. J. Humphreys, *Appl. Phys. Lett.* **93**, 101901 (2008).
- ¹⁷A. Dussaigne, P. Corfdir, J. Levrat, T. Zhu, D. Martin, P. Lefebvre, J.-D. Ganière, R. Butté, B. Deveaud-Plédran, N. Grandjean, Y. Arroyo, and P. Stadelmann, *Semicond. Sci. Technol.* **26**, 025012 (2011).
- ¹⁸T. Akiyama, T. Yamashita, K. Nakamura, and T. Ito, *Nano Lett.* **10**, 4614 (2010).
- ¹⁹P. Corfdir, B. Van Hattem, E. Uccelli, A. Fontcuberta i Morral, and R. T. Phillips, *Appl. Phys. Lett.* **103**, 133109 (2013).
- ²⁰M. De Luca, G. Lavenuta, A. Polimeni, S. Rubini, V. Grillo, F. Mura, A. Miriametro, M. Capizzi, and F. Martelli, *Phys. Rev. B* **87**, 235304 (2013).
- ²¹N. Vainorius, S. Lehmann, A. Gustafsson, L. Samuelson, K. A. Dick, and M.-E. Pistol, *Nano Lett.* **16**, 2774 (2016).
- ²²K. P. O'Donnell, R. W. Martin, and P. G. Middleton, *Phys. Rev. Lett.* **82**, 237 (1999).
- ²³J. Even and S. Loualiche, *J. Phys. A: Math. Gen.* **37**, L289 (2004).
- ²⁴M. G. A. Bernard and G. Duraffourg, *Phys. Status Solidi B* **1**, 699 (1961).
- ²⁵L. Sirigu, D. Y. Oberli, L. Degiorgi, A. Rudra, and E. Kapon, *Phys. Rev. B* **61**, R10575 (2000).